sciendo

POLISH MARITIME RESEARCH 2 (106) 2020 Vol. 27; pp. 39-47
10.2478/pomr-2020-0025

PARAMETERS IDENTIFICATION OF THE FLEXIBLE FIN KINEMATICS MODEL USING VISION AND GENETIC ALGORITHMS

Karolina Jurczyk
Polish Naval Academy, Poland
Paweł Piskur
Polish Naval Academy, Poland
Piotr Szymak
Polish Naval Academy, Poland

ABSTRACT

Recently a new type of autonomous underwater vehicle uses artificial fins to imitate the movements of marine animals, e.g. fish. These vehicles are biomimetic and their driving system is an undulating propulsion. There are two main methods of reproducing undulating motion. The first method uses a flexible tail fin, which is connected to a rigid hull by a movable axis. The second method is based on the synchronised operation of several mechanical joints to imitate the tail movement that can be observed among real marine animals such as fish. This paper will examine the first method of reproducing tail fin movement. The goal of the research presented in the paper is to identify the parameters of the one-piece flexible fin kinematics model. The model needs further analysis, e.g. using it with Computational Fluid Dynamics (CFD) in order to select the most suitable prototype for a Biomimetic Underwater Vehicle (BUV). The background of the work is explained in the first section of the paper and the kinematic model for the flexible fin is described in the next section. The following section is entitled Materials and Methods, and includes a description of a laboratory test of a water tunnel, a description of a Vision Algorithm (VA)which was used to determine the positions of the fin, and a Genetic Algorithm (GA) which was used to find the parameters of the kinematic fin. In the next section, the results of the research are presented and discussed. At the end of the paper, the summary including main conclusions and a schedule of the future research is inserted.

Keywords: Biomimetic Underwater Vehicle,flexible fin kinematics model,parameters identification using vision,Genetic Algorithm

INTRODUCTION

Biomimetic Underwater Vehicles (BUVs), like classical Autonomous Underwater Vehicles (AUVs), can be used in a wide variety of underwater applications such as monitoring, the investigation of a sea region, pollution detection, military operations and protection [14, 15]. The undulating propulsion system is being developed by scientific teams around the world and is becoming more popular in new designs of autonomous underwater vehicles [14]. This is due to the advantages of the undulating propulsion system, like its highly efficient locomotion and manoeuvring in water. Propulsion systems with rotary propellers have energy efficiency limited to 70% and they are 20% less efficient than the swimming mechanism of real fish [6]. What is more, the rotary propulsion system is noisier and less manoeuvrable than the bio-inspired system. Due to their shape and outer appearance, BUVs can operate more secretly than AUVs. This feature is important not only for military applications but also for civilian uses, e.g. for the inspection of underwater fauna.

Fig. 1 depicts three kinds of fish tail. The shape of the fins has a large influence on their efficiency [8], but the interaction with the undulating flexible body and the passive response of the fluid forces are still poorly understood [21, 22] and scientific research in this domain has mainly been done using empirical methods.

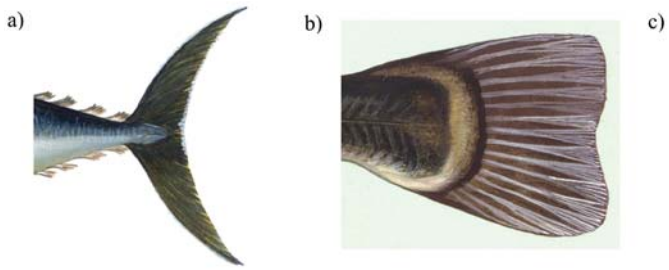

Fig. 1. The shape of the fish tail of: a) a tuna, b) a catfish, c) a shark

BUVs have been under investigation for almost ten years in Cracow University of Technology [12] and the Polish Naval Academy [18]. The first mentioned research team built a BUV with an undulating propulsion system based on the connection of the rigid bodies (Fig. 2), while the second research team was focused on a flexible tail fin (Fig. 3). The analysis of a travelling wave's impact on the speed of the BUV with a tail fin created from joined multiple rigid bodies was presented in [12]. The undulating propulsion measurements of an artificial fish with one tail fin and an artificial seal with two tail fins were presented in [17]. In [6], a fish-like swimming robot was presented based on the behaviour of carp.

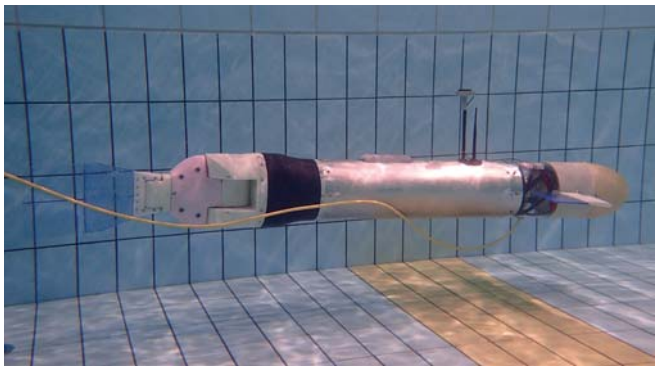

Fig.2. The BUV with two side fins and one tail fin as a chain of interconnected links [14]

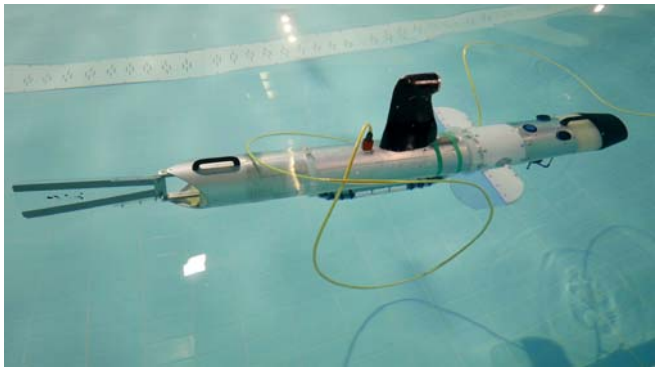

Fig. 3. The BUV with two side fins and one tail flexible fin [17]

Although many links are needed to accurately reproduce fish-like behaviour, this makes implementation and control of the robot more complicated. In addition, the increasing number of tail segments increases the likelihood of water leakage from the connection areas, which can lead to the destruction of the sensitive electronic components inside, and even submerge the vehicle. The cost rises significantly if a swarm of artificial fishes is taken into consideration. For these reasons, it was assumed that the fish movement should be reproduced by a one-piece flexible fin with a motor shaft mounted on the leading edge of the fin.

This approach demands the selection of the proper fin for imitation of the desired motion. A proper fin means not only the structural parameters of the fin, such as shape, dimensions, and stiffness, but also control parameters such as the frequency of oscillation, maximal deflection and even the type of the function of the fin motion [1]. In the opinion of the authors, the designed method for identifying the parameters of the flexible fin kinematics model (presented in the next part of the paper) can significantly shorten the time taken to achieve the final effect in the form of the proper fin selection for the BUV. Such fins can be used in the BUV as a tail fin or a pectoral fin, depending on the selected propulsion system.

In the following section, the mathematical description of the tail fin kinematics is presented. Then, the laboratory test stand of a water tunnel is described, and the VA and the GA optimisation respectively for determining the fin deflection and identifying the kinematics model parameters are depicted. Next, the results of research including both the subsequent determination of the fin positions and the identification of the fin kinematics model parameters using GA are presented. At the end of the paper, the conclusions and foreseen research are included.

KINEMATICS OF CAUDAL FLEXIBLE FIN

Considering the physiology and biomechanics of fish [16], two different types of undulating propulsion can be distinguished:

1. Median and/or Paired Fin propulsion (MPF) consisting of even, symmetric abdominal or breast fins, or the dorsal and/or anal fins. Species of fish belonging to the mentioned families are characterised by much lower manoeuvrability and speed in relation to fish moving with the use of a tail fin. Thus, the construction of robots imitating the above-mentioned life forms will be characterised by similar features.
2. Body and/or Caudal Fin propulsion (BCF) using a coordinated movement of the body and caudal fin, or only movement of the caudal fin. Species of fish that move in this way are characterised by much faster speed and manoeuvrability in relation to the MPF fishes [10].

In [20] the comparison between MPF and BCF is included. In this paper, the most popular BCF is considered [11]. The

description of BCF fish body motion, originally proposed by Lighthill [9], approximates the travelling wave (Fig. 4) by the composition of polynomial and sinusoidal curves:

$$y(x,t) = (c_1 x + c_2 x^2)\sin(kx + \omega t) \quad (1)$$

where:
$y(x,t)$ – the transverse displacement of the tail unit;
x – the independent spatial variable;
t – time, a second independent variable;
c_1 – the primary coefficient of the fish wave envelope;
c_2 – the quadratic term coefficient of the fish wave envelope;
$k = 2\pi/\lambda$ – the wave number;
λ – the wavelength of the fish body;
$\omega = 2\pi f$ – the frequency of the fish wave.

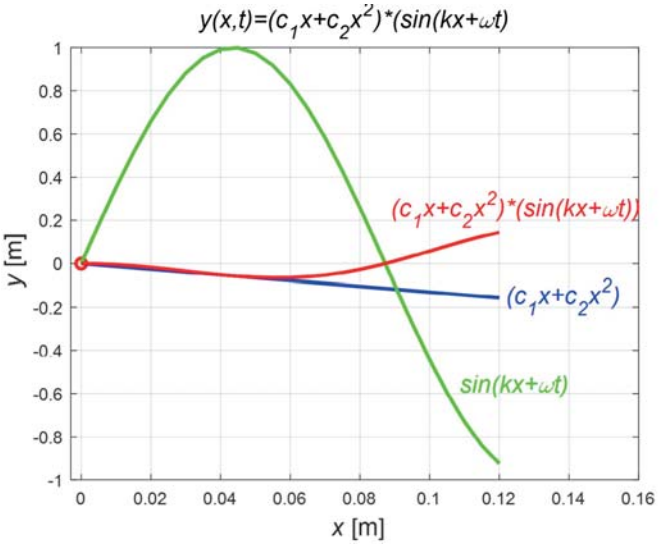

Fig. 4. The fin undulating wave curve for discrete time and constant coefficients

The coefficients (c_1, c_2, k) in Lighthill's model and the wave parameters of moving fish vary depending on the type of fish analysed and its kinetic status in water [23]. In Fig. 4, Eq. (1) is presented for discrete time and for the constant coefficients.

In [7] and [12], the optimisation of the traditional kinematic model by introducing the head swinging equation and the swinging centre offset is presented, but the equation coefficients are still unknown and need to be identified.

METHODS AND MATERIALS

THE LABORATORY TEST STAND

The tests were carried out on the laboratory test stand depicted in Fig. 5. Different types of flexible fins were driven by the servomechanism (Dynamixel AX-12+) with a maximum torque of 1.5 Nm. The servomechanism is mounted on a transparent polycarbonate plate with ball bearings. The wave drive parameters needed to determine the deflection of the fin and identify the equation parameters were recorded using a vision system. Measurements of the generated driving force can be realised by means of precision strain gauges mounted on both sides of the water channel. The additional forced fluid flow is carried out by means of an external pump with different fluid velocity. The fluid velocity is measured by a non-invasive method using an ultrasonic flowmeter.

Fig. 5. The laboratory test stand: 1 – PC, 2 – microcontroller unit, 3 – servomotor, 4 – fin, 5 – strain gauges, 6 – ball bearings, 7 – external water pump, 8 – ultrasonic flow meter, 9 – linear laser

The relationship between the three-dimensional wake created by different fin shapes and performance is very difficult to determine using the simulation model [2], which is why the vision system was implemented. The designed laboratory test stand gives the opportunity to analyse fin kinematics for a wide range of shapes and construction parameters. At the beginning, the rectangular fins were tested, followed by tuna fins (Fig. 6). The developed method will be used for assessing the impact of particular dimensions presented in Fig. 6 (L, h, w, $R1$, $R2$, $R3$, $R4$) on the coefficients c_1, c_2, and k in the equation of the kinematics model (1).

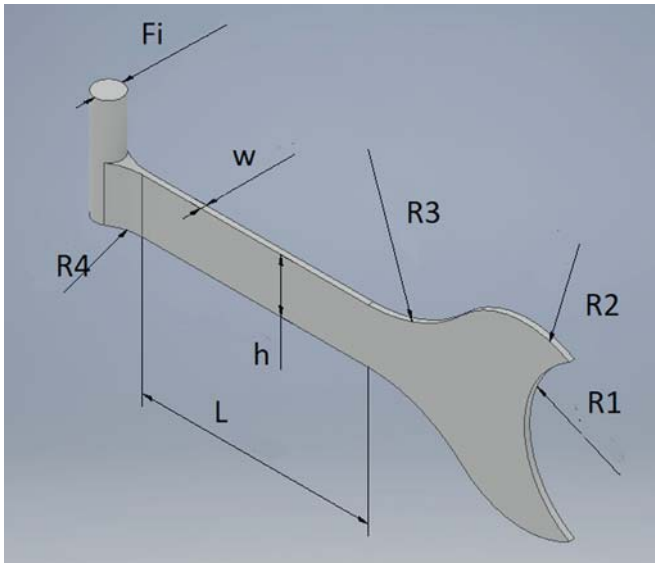

Fig. 6. Dimensions of tuna-shape fin

Deflection of the fin was measured with a camera placed in the top view of the water channel. A sample image with a tuna-shape fin is shown in Fig. 7.

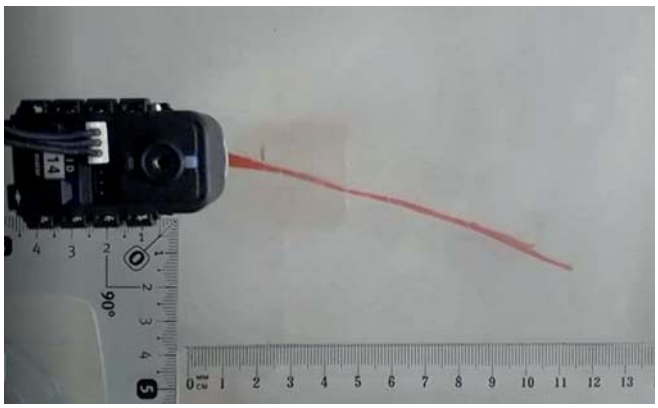

Fig. 7. Top view of tuna-shape fin during experiments

In the designed laboratory test stand the vision system is calibrated and methods are developed for comparison of the one-piece fin kinematics with real fish behaviour. Moreover, in the laboratory test stand the propulsion force can be measured and fluid-structure interaction can be investigated in greater depth using the Particle Imaginary Velocimetry method (PIV).

VA FOR FIN DEFLECTION DETERMINATION

During the research using the Vision Algorithm (VA), a video camera with the following parameters was used: 8 MP, f/2.4, 31 mm, AF with embedded correction of the optical distortion, and the following video recording parameters were applied: 1920 x 1080 pixels resolution with 30 frames per second.

To design the VA, the classical video images processing methods were adopted. The designed VA consists of the following stages:

1. Selection from the movie of the frames containing a full cycle of the fin motion.
2. Image filtration using colour thresholding with additional binarisation.
3. Mapping pixels of the image into the points in the Cartesian coordinate system.

At the beginning, the frames including a full cycle of the fin motion were selected. The full cycle began from the zero position of the servomechanism, i.e. the fin was positioned in the longitudinal axis of the tunnel symmetry. The servo worked to the right maximal deflection and then worked to the left maximal deflection. The full cycle of the fin motion ended in the zero position of the servomechanism. The number of frames was dependent on the frequency of the fin oscillation. Fig. 8a visualises an example of the frames.

The goal of the next stage of the VA was to isolate the red fin from the background of the image. This was done using colour thresholding [4, 5]. Due to the fact that some pixels of the surface water located close to the fin also had a quite large level of the red colour value, similar to the fin, the additional binarisation operation was applied. The effect of the operation is indicated in Fig. 8b.

The third stage of the VA was dedicated to mapping the pixels of the images into the points in the Cartesian coordinate system. After the calibration process, it was accepted that 69 pixels correspond to 0.01 m distance. An example result of this stage is illustrated in Fig. 8c.

In order to plot the curve function corresponding to the deflection of the fin, a polynomial curve was determined. The coefficients of the n^{th} degree polynomial were found using a least-squares method that best fits the data from the vision system. Based on the data analysis, it was decided that the best curve fit gives a polynomial degree equal to 18, because lower values caused matching errors, and higher values of the polynomial degree did not yield a better result. Then the polynomial function was used to obtain values of coordinate y for selected values of coordinate x. The values received from the polynomial function are reference values, because they were obtained from the real fin oscillation in the water tunnel.

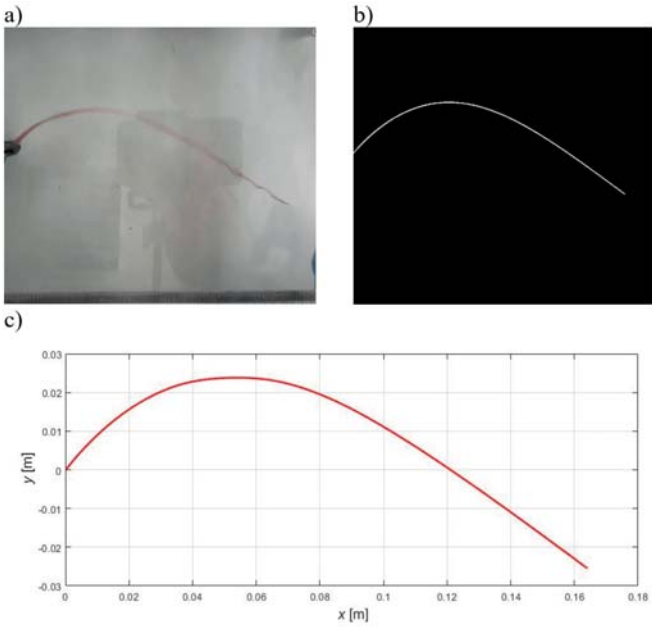

Fig. 8. The following stages of image processing: a) the source image, b) the binary image, c) the image in the Cartesian coordinate system

As the final result of the VA, the mapping points in the Cartesian coordinate system were determined. The points were selected every 0.01 m distance in the x axis. In the first step of analysis, the parameter optimisation was done for every frame separately, then the analysis was performed for the full cycle. It is worth underlining that the full cycle consists of different numbers of frames depending on the frequency of oscillation. The details of the optimisation are included in the next subsection.

GA FOR FIN MODEL PARAMETERS IDENTIFICATION

The fluid structure interaction is a strongly nonlinear phenomenon [19], which is why the genetic algorithm (GA) was used [13, 24]. The goal of the GA is to find optimal values of the following parameters of the flexible fin kinematics model included in formula (1): c_1, c_2, k. The range of the decision variables (c_1, c_2 and k) and the nonlinearity of the kinematic model lead to the application of probabilistic algorithms.

The space for potential solutions in matching the searched for coefficients c_1, c_2 and k of the travelling wave equation is so large that it is not possible in a sufficiently short time to check all possible options in order to find the best solution. Therefore, it is justified to use probabilistic techniques based on random selection. One such technique is the genetic algorithm, which has been successfully used in the experiment.

In general, the GA is a heuristic search that mimics the process of natural selection. The GA is based on an iterative evolutionary procedure involving the selection of genotypes for reproduction based on their fitness, and then introducing genetically changed (by means of a mutation, a crossover and other genetic operators) offspring into the next population. The procedure ends after achieving satisfactory genotypes (a set of features of an individual) which correspond to phenotypes with the highest fitness function (the individual from a population) [3].

During the GA optimisation of the fin model parameters, the initial population was generated using a random generator. A population consisting of 15 individuals was accepted. The next generation of the population was computed using the following fitness function of the individuals in the current generation:

$$f_{fitness} = \sum_{i=1}^{n}\sum_{j=1}^{m}\left|y_y(x_j(i)) - y_k(x_j(i))\right| \quad (2)$$

where:
$y_y(x_j(i))$ – the coordinate y achieved from the vision system for the i-th fin position (the i-th frame taken in the discrete time) and j-th value of coordinate x;
$y_k(x_j(i))$ – the coordinate y for the i-th fin position and j-th value of coordinate x achieved using the travelling wave equation (1) in the following discrete form:
$y_k(x_j(i)) = (c_1 x_j(i) + c_2 x_j(i)^2)\sin(kx_j(i) + \omega i)$;
n – the number of fin positions taken in the following discrete time steps;
m – the number of discrete values of coordinate x taken into consideration.

After calculation of the fitness function, a reproduction algorithm creates children for the next generation. In the reproduction, the following operators were used:

- Rank fitness scaling.
- Stochastic uniform selection function.
- Crossover fraction equal to 0.8.
- Gaussian mutation equal to 0.2.

The fitness scaling converts the raw fitness scores that are returned by the fitness function to values in a range that is suitable for the selection function. The rank fitness scaling scales the raw scores based on the rank of each individual instead of its score. The rank of an individual is its position in the sorted scores. An individual with the rank r has a scaled score proportional to $1/\sqrt{r}$.

The selection function specifies how the genetic algorithm chooses parents for the next generation. The stochastic uniform selection function lays out a line in which each parent corresponds to a section of the line of length proportional to its scaled value. The algorithm moves along the line in steps of an equal size. At each step, the algorithm allocates a parent from the section it lands on. The first step is a uniform random number less than the step size.

The crossover fraction specifies the fraction of the next generation, other than elite children, that are produced by the crossover, while the Gaussian mutation adds a random number taken from a Gaussian distribution with the mean 0 to 0.2 part of the parent vector.

During the research, the GA used the following criteria for stopping the algorithm:

- The maximum number of 500 generations is reached.
- The detection of no change in the best fitness function value for a maximum 10 stall generations is achieved.

The upper and lower limits of the parameters searched for were obtained from the literature on fish behaviour [8, 9]. The positive value of lambda was assumed.

RESULTS AND DISCUSSION

The different shapes of the fins were taken into consideration. The servomotor moved the fin with the frequency f of up to 2 Hz and the angle A_{max} of up to 60°. The fin deflection depends on the length, the width and the shape of the fin as well.

For one discrete position of the fin, the GA divergence as a function of the iteration number is presented in Fig. 9. The identification of the unknown coefficients from Eq. (1) was performed in over 100 iterations (Figs. 10–12), while for the full cycle of the fin movement (Figs. 13–14) more than 300 iterations were generated.

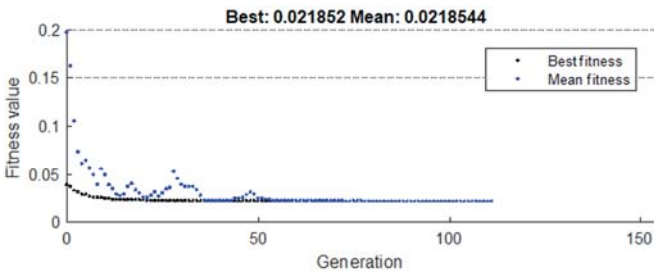

Fig. 9. Fitness value as a function of iteration number

The experimental results achieved from the VA are presented in the red colour in Figs. 11–12. The simulation results for discrete time are presented using blue lines.

The simulation tests were performed for the parameters achieved from the identification process using the GA.

The first experiment (Fig. 11) was conducted for a rectangular-shaped fin made from polypropylene (Young's modulus equal to 1.75 GPa) oscillating with f = 1.8 Hz and dimensions: L = 0.2 m, h = 0.015 m, w = 0.002 m. Fig. 10 presents the comparisons between the simulation and experiment (a) during and (b) after finishing the optimisation process. The coefficients evaluated by the GA are c_1 = 0.72 and c_2 = -6.5, while the λ ($k = 2pi/\lambda$) depends on the fluid velocity and changes from λ = 9 (v_{fluid} = 0 m/s) to λ = 0.7 (v_{fluid}=0.3 m/s).

The second experiment depicted in Fig. 12 was performed for a tuna-shaped fin made of acrylic glass and dimensions: L = 0.12 m, h = 0.015 m, w = 0.002 m, R1 = 0.05 m, R2 = 0.75, R3 = 0.05 m, for a sequence of discrete positions over time (fin oscillating with f = 1.5 Hz). The coefficients evaluated by the GA are the following: c_1 = 0.46 and c_2 = -0.3, while the λ ($k = 2pi/\lambda$) changes from λ = 140 (v_{fluid} = 0 m/s) to λ = 17 (v_{fluid} = 0.3 m/s).

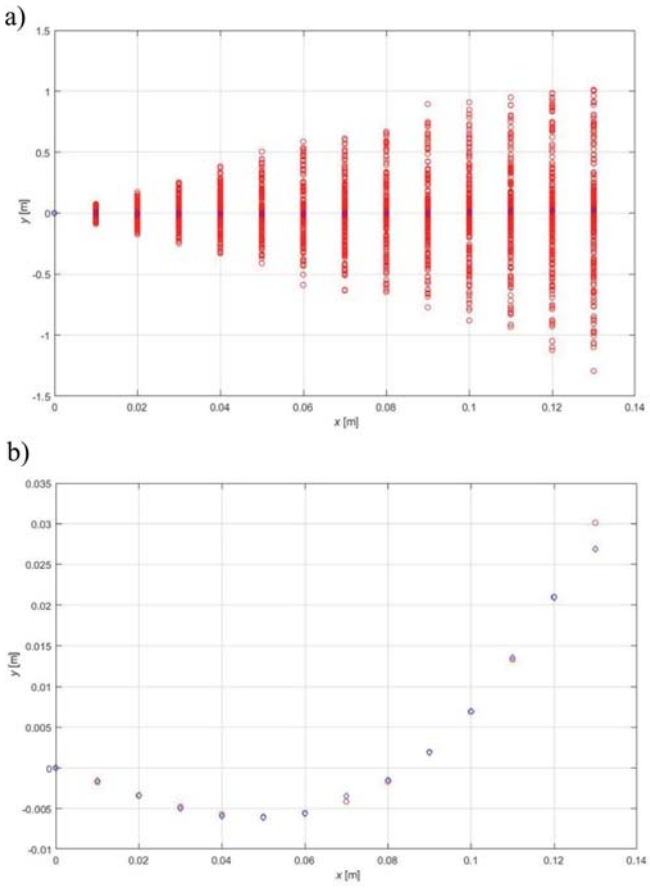

Fig. 10. Fig. 10. Position of the following points of the fin achieved from vision system (blue diamonds) and from fin model (red circles) in the following steps of tha GA operation (a) and after finding optimal solution (b)

As shown in Fig. 10, the results of the experiment obtained from the visual system are well-matched compared with the simulation results. The value of the fitness function was lower than 0.75 [%]. Therefore it can be concluded that the presented VA is sufficient for the subsequent research.

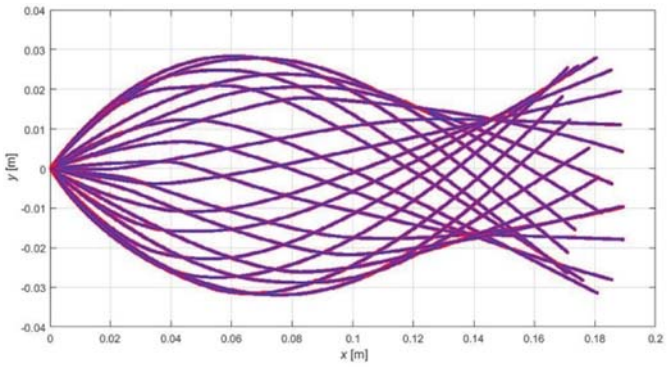

Fig. 11. The deflection of the rectangular-shaped fin in the discrete time obtained from the vision system (red markers) and from the kinematics model (blue lines)

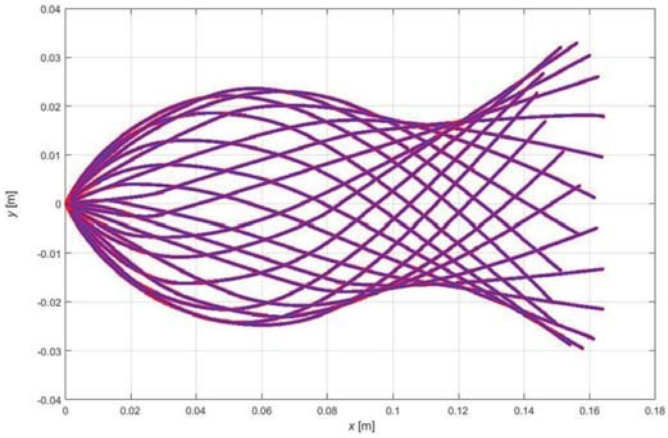

Fig. 12. The deflection of the tuna-shaped fin in the discrete time obtained from the vision system (red markers) and from the kinematics model (blue lines)

In the next step, the GA was used to estimate unknown parameter values in the fin kinematics model for the full fin movement cycle. Fig. 13 presents the fin deflection (y_y) for the full cycle in the i-th discrete time. For the servomotor frequency motion equal to 1.6 Hz, the sequence of 19 frames was achieved from the vision system (Fig. 13). Then, the GA with Eq. (2) was used for estimation of the unknown parameter values. For the estimated value the simulation was conducted. The results of the simulation in the form of the fin deflection for the i-th discrete time are presented in Fig. 14. In order to verify the simulation data with the experimental ones, the following formula was used:

$$\Delta y\left(x_j(i)\right) = \frac{y_y\left(x_j(i)\right) - y_k(x_j(i))}{\frac{f_{fitness}}{n * m}} \tag{3}$$

where:
$y_y(x_j(i))$ – the coordinate y for the i-th fin position (the i-th frame taken in the discrete time) and j-th value of coordinate x achieved from the vision system (Fig. 13);

$y_k(x_j(i))$ – the coordinate y for the i-th fin position and j-th value of coordinate x achieved using the travelling wave equation (1);
$f_{fitness}$ – the fitness function obtained using Eq. (2);
n – the number of fin positions taken in the following discrete time steps;
m – the number of discrete values of coordinate x taken into consideration.

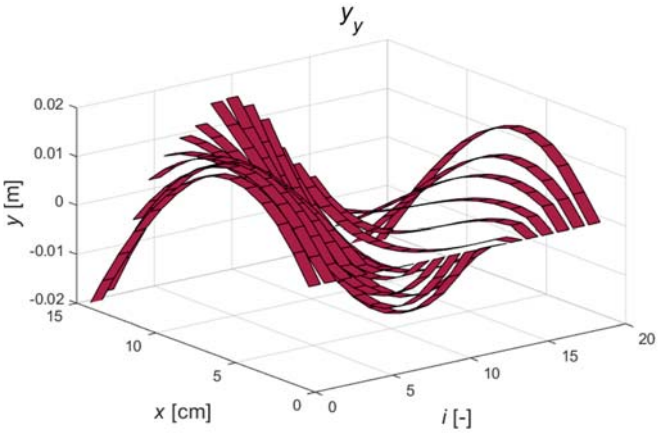

Fig. 13. The fin deflection in the i-th discrete time measured by the VA

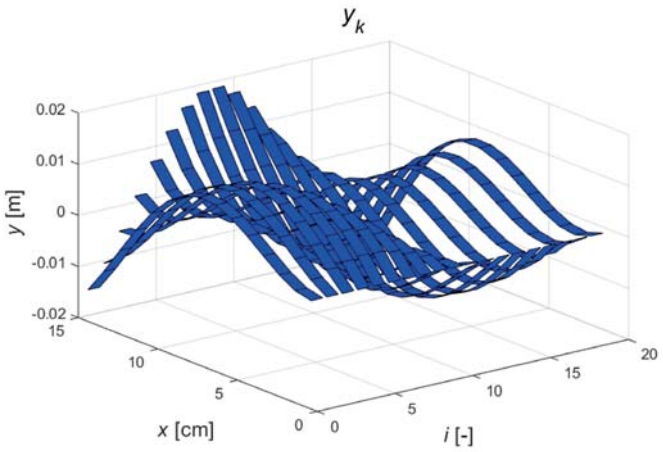

Fig. 14. The fin deflection in the i-th discrete time achieved from the simulation with optimised coefficients

The result of the method verification according to Eq. (3) for the rectangular-shaped fin is presented in Fig. 15. For every fin position in discrete time the error is compared to the value of the fitness function from the GA. The coefficients evaluated by the GA are: $c_1 = 0.48$ and $c_2 = -0.65$, while the λ ($k = 2pi/\lambda$) changes from $\lambda = 7.8$ ($v_{fluid} = 0$ m/s) to $\lambda = 0.63$ ($v_{fluid} = 0.3$ m/s).

The mean value of the relative error does not exceed 3%. To summarise, it is possible to find out the coefficients of Eq. (1) for the undulating propulsion kinematics model with sufficient accuracy. Then, the dimension of the fin can be modified and the kinematics can be compared to real fish movement.

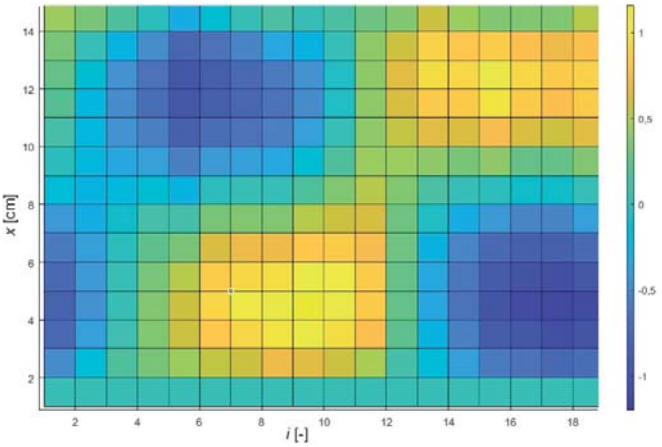

Fig. 15. Graph of differences between the results from the vision system and from the simulation model

SUMMARY

Fin kinematics depends on a combination of many non-linear factors. Therefore, an experimental method was selected to analyse the impact of the construction parameters on the deflection of the fin. Although the structure–fluid interaction is strongly non-linear, the presented method (VA + GA) gives the values of the kinematics equation parameters with the desired accuracy.

The designed algorithm provides the opportunity to establish the positions of the fin in different time steps and different spatial coordinates. The presented method of identifying the parameters of the undulating kinematics model allows us to assess the compatibility of the model coefficients with selected fish species. Afterwards, the use of the GA allows us to find the non-dominant minimum of the fitness function, and finally the searched for values of the decision variables.

Therefore, in summary, the construction data can be analysed, and the influence of the shape factor on the fin kinematics can be studied using the proposed VA and GA. Moreover, a more sophisticated control algorithm can be implemented for the desired fin deflection.

In the laboratory test stand, the propulsion force can be measured and the fluid–structure interaction can be investigated in greater depth using the PIV method, which will be used in further studies.

The presented algorithm can also be used during tests in a large water reservoir, where a vision system is used to record tail deflection.

ACKNOWLEDGEMENT

The paper is supported by the Research Grant of the Polish Ministry of Defence entitled "Model studies of the characteristics of an undulating propulsion system".

REFERENCES

1. Chen Z., Shatara S., Tan X. (2010): *Modelling of biomimetic fish propeller by an ionic polymer-metal caudal fin*. IEEE/ASME Transactions on Mechatronics, Vol. 15(3), 448-459.

2. Graaf V. (2018): *Final report Biomimetic Propulsion*.

3. Goldberg D. E. (1989): *Genetic Algorithms in Search, Optimization and Machine Learning*, Addison-Wesley Longman Publishing, Boston.

4. Hożyń S., Żak B. (2015): *Moving object detection, localization and tracking using stereo vison system.* Solid State Phenomena, Vol. 236, 134-144.

5. Hożyń S., Żak B. (2017): *Local image features matching for real-time seabed tracking applications.* Journal of Marine Engineering and Technology, Vol. 16, 273-282.

6. Koca G. O., Bal C., Korkmaz D. (2018): *Three-dimensional modeling of a robotic fish based on real carplLocomotion*. Applied Sciences, Vol. 8, 180.

7. Korkmaz D., Budak U., Bal C. (2012): *Modeling and implementation of a biomimetic robotic fish*. IEEE Conference, doi: 10.1109/SPEEDAM.2012.6264510

8. Krishnadas A., Ravichandran S., Rajagopal P. (2018): *Analysis of biomimetic cadual fin shapes for optimal propulsive efficiency.* Ocean Engineering, Vol. 153, 132-142.

9. Lighthill M. J. (1960): *Note on the swimming of slender fish.* Journal of Fluid Mechanics, Vol. 9, 305-317.

10. Liu J., Hu. H. (2010): *Biological inspiration: From carangiform fish to multi-joint robotic fish.* Journal of Bionic Engineering, Vol. 7, 35-48.

11. Lou B., Ni Y. Mao M., Wang P., Cong Y. (2017): *Optimization of the kinematic model for niomimetic robotic dish with rigid headshaking sitigation.* Robotics, Vol. 6, 30, doi:10.3390/robotics6040030.

12. Malec M., Morawski M., Szymak P., Trzmiel A. (2013): *Analysis of parameters of traveling wave impact on the speed of biomimetic underwater vehicle.* Solid State Phenomena, Vol. 210, 273-279.

13. Mathworks (2018): *MATLAB documentation*, https://www.mathworks.com/help/gads/how-the-genetic-algorithm-works.html.

14. Morawski M., Słota A., Zając J., Malec M., Krupa K. (2017): *Hardware and low-level control of biomimetic underwater vehicle designed to perform ISR tasks.* Journal of Marine Engineering & Technology, Vol. 16, 227-237.

15. Piskur P., Szymak P. (2017): *Algorithms for passive detection of moving vessels in marine environment.* Journal of Marine Engineering & Technology, Vol. 16, 377-385.

16. Shadwick R., Lauder G. (2006): *Fish Physiology: Fish Biomechanics*, Vol. 23. Academic Press.

17. Szymak P., Praczyk T., Naus K., Szturomski B. (2016): *Research on biomimetic underwater vehicles for underwater ISR.* Ground/Air Multisensor Interoperability, Integration, and Networking for Persistent ISR VII, 2016, doi: 10.1117/12.2225587.

18. Szymak P., Przybylski M. (2018): *Thrust measurement of biomimetic underwater vehicle with undulating propulsion.* Scientific Journal of Polish Naval Academy, Vol. 213(2), 69-82.

19. Taylor G. K., Nudds R. L., Thomas A. L. (2003):. *Flying and swimming animals cruise at a Strouhal number tuned for high power efciency.* Nature, Vol. 425, 707-710.

20. Tey W., Sidik N. (2015): *Comparison of swimming performance between two-dimensional carangiform and anguilliform locomotor.* Advanced Research in Fluid Mechanics and Thermal Sciences, Vol. 11(1), 1-10.

21. Tytell E., Hsu C., Fausi L. (2014): *The role of mechanical resonance in the neural control of swimming in fishes.* Zoology (Jena), Vol. 117(1), 48-56.

22. Tytell E., Lu. M. (2016): *Role of body stiffness in undulatory swimming: Insights from robotic and computational models.* Physical Review Fluids, Vol. 1.

23. Wang J., Tan X. (2015): *Averaging of tail-actuated robotic fish dynamics through force and moment scaling.* IEEE Transactions on Robotics, Vol. 31(4), 906-917.

24. Weise T. (2009): *Global Optimization Algorithms - Theory and Application*, Retrieved: http://www.it-weise.de/

CONTACT WITH THE AUTHORS

Karolina Jurczyk
e-mail: k.jurczyk@amw.gdynia.pl

Polish Naval Academy,
Smidowicza 69, 81127 Gdynia,
Poland

Paweł Piskur
e-mail: p.piskur@amw.gdynia.pl

Polish Naval Academy,
Smidowicza 69, 81127 Gdynia,
Poland

Piotr Szymak
e-mail: p.szymak@amw.gdynia.pl

Polish Naval Academy,
Smidowicza 69, 81127 Gdynia,
Poland